ID 4228408025). Bilinear interpolation was used in resampling, and geometric correction resulted in 58-m rms error for the 1972 scene, 114-m rms error for the 1986 scene, and 41-m rms error for the 1988 scene. Overlay of the images in areas of bedrock ridges indicates that the registration is accurate to 1 to 2 pixels, although even in these areas, sand accumulations in the lee of bedrock ridges could make the coregistration appear worse than it actually is.

6. We converted the image data to spectral radiance following procedures outlined in B. L. Markham and J. L. Barker, [*Landsat Technical Notes 1* (Earth Observation Satellite Company, Lanham, MD, 1986)], in which

$$L_\lambda = LMIN_\lambda + \frac{LMAX_\lambda - LMIN_\lambda}{QCALMAX} QCAL$$

where L_λ is spectral radiance of band λ (in milliwatts per square centimeter per steradian per micrometer), *LMIN* and *LMAX* are calibrated spectral radiances used in ground processing, *QCALMAX* is the range of radiance values, and *QCAL* is the quantized scaled radiance value (*dn*) of the Landsat data. Exoatmospheric reflectance, ρ_p, was calculated by

$$\rho_p = \frac{\pi \ L_\lambda \ d^2}{ESUN_\lambda \ \cos\theta_s}$$

where *d* is the Earth-sun distances (in astronomical units), *ESUN* is mean solar exoatmospheric reflectance (milliwatts per square centimeter per micrometer), and θ_s is solar zenith angle. Markham and Barker suggested that uncertainties in exoatmospheric reflectance resulting from sensor changes with time are less than 2% for the MSS instruments.

7. The brightness values thus calculated are essentially exoatmospheric reflectances, and although variation in reflectance between the scene dates can be caused by variations in aerosol composition, we assume that this composition was constant. Air temperature averaged 15° to 20°C at 0930 an (nominal Landsat pass time), and relative humidity was 20 to 30%. Sandstorms, which would completely obscure the surface from satellite observations, rarely occur from November to February.
8. A negative transparency from June 1985 was overlain on 1:1,000,000 prints from October 1984 and January 1986, and in each case, matching the chevron patterns produced offsets in the dunefield to the west, and in bedrock exposures north of the sand sheet. We found this method of matching the chevron patterns and looking for changes in stable features more accurate than the reverse because there are only a few stable landforms in the region. When doing this, we noted no changes in the patterns of the chevrons, suggesting short-term (yearly) movement of the features as discrete bedforms.
9. The fine- to coarse-sand particles are dominantly iron oxide–coated quartz grains derived from the Nubian sandstone prevalent throughout the Western Desert of Egypt.
10. R. L. Folk, in *Proc. Intl. Geol. Cong. 23rd Session* (Academia, Prague, 1968), pp. 9–32; T. A. Maxwell, in *Desert Landforms of Southwest Egypt: A Basis for Comparison with Mars*, F. El-Baz and T. A. Maxwell, Eds. (Contractors Rep. 3611, National Aeronautics and Space Administration, Washington, DC, 1982), pp. 157–173.
11. R. Greeley and J. D. Iverson, *Wind as a Geological Process* (Cambridge Univ. Press, Cambridge, 1985), pp. 149–155; I. G. Wilson, *Sedimentology* **19**, 173 (1972).
12. Bedform migration rate as defined by D. M. Rubin and R. E. Hunter [*Sedimentology* **29**, 121 (1982)] is:

$$i = VHk$$

in which *i* is transport rate (volume per unit time per unit width), *V* is the rate of bedform migration, *H* is the bedform height, and *k* is cross-sectional area divided by wavelength divided by height.

13. We thank K. Katzer, B. Gillespie, and E.-S. Zaghlool for their assistance in surveying, and the General Petroleum Company, Egypt for logistical assistance during early phases of this study. This study was supported by National Science Foundation grants EAR-8312651 and EAR-8607479, National Geographic Society grant 2790-84, and Smithsonian Foreign Currency grant FC10215300 to C. V. H. and by the National Air and Space Museum, Smithsonian Institution to T. A. M. We thank P. A. Jacobberger, S. Soter, C. S. Breed, and two anonymous reviewers for their reviews of this manuscript.

31 August 1988; 22 December 1988

Stishovite at the Cretaceous-Tertiary Boundary, Raton, New Mexico

JOHN F. MCHONE, RONALD A. NIEMAN, CHARLES F. LEWIS, ANN M. YATES

Stishovite, a dense phase of silica, has become widely accepted as an indicator of terrestrial impact events. Stishovite occurs at several impact structures but has not been found at volcanic sites. Solid-state silicon-29 magic-angle spinning nuclear magnetic resonance (silicon-29 MAS NMR) and X-ray diffraction of samples from the Cretaceous-Tertiary boundary layer at Raton, New Mexico, indicate that stishovite occurs in crystalline mineral grains. Stishovite was indicated by a single, sharp resonance with a chemical shift value of −191.3 ppm, characteristic of silicon in octahedral coordination, that disappeared after heating the sample at 850° Celsius for 30 minutes. An X-ray diffraction pattern of HF residuals from the unheated sample displayed more than 120 peaks, most of which correspond to quartz, zircon, rutile, and anatase. Eight unambiguous weak to moderate reflections could be ascribed to *d*-spacings characteristic of stishovite.

SINCE ALVAREZ *et al.* (*1*) SUGGESTED that an extraterrestrial impact was the cause of Cretaceous-Tertiary (K-T) extinctions, mineral grains showing multiple sets of shock lamellae have been discovered in weakly indurated sediments from the K-T boundary (*2*) at numerous locations around the world (*3*). Although such features were thought to be indicative of violent impact events, several workers have recently suggested that shocked mineral grains can also originate during explosive volcanism (*4*). The mineral stishovite, another strong indicator of shock history, does not survive near-surface exposure to volcanic temperatures. Therefore, detection of stishovite would indicate that shock effects observed in K-T boundary sediments were due to meteoritic impact, rather than volcanic eruption.

Quartz, a common mineral in the earth's crust, is a silica (SiO_2) polymorph with silicon in tetrahedral coordination with oxygen. At pressures of 3.5 GPa, quartz converts to coesite, a dense, tetrahedrally-coordinated monoclinic polymorph. At pressures greater than 8.5 GPa, stishovite forms (*5*). Stishovite is an even denser, tetragonal polymorph, with silicon in octahedral coordination with oxygen. Stishovite can also form from zircon, which decomposes to ZrO_2 and SiO_2 at pressures above 22 GPa (*6*). Once formed, stishovite is metastable at atmospheric pressure and moderate temperature and reverts to other silica polymorphs when heated (*7*). Natural stishovite has been found only in rock samples from known or suspected meteoroid impact sites and is considered diagnostic of impact-induced shock metamorphism (*8*).

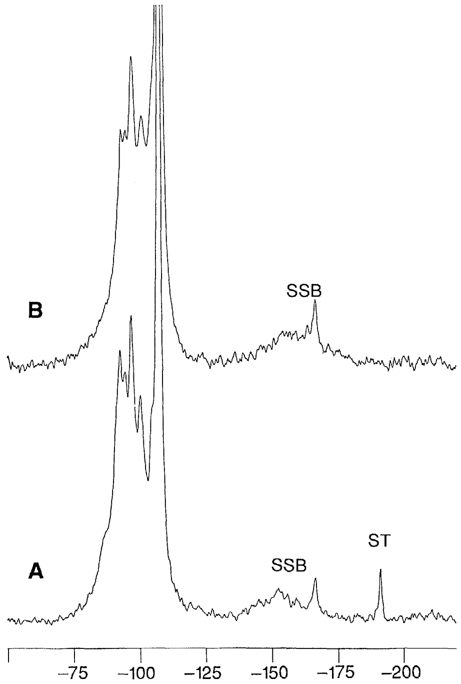

Fig. 1. ^{29}Si MAS NMR spectra of K-T boundary mineral grains (*16*). (**A**) Residual K-T boundary grains isolated by sedimentation, magnetic separation and HNO_3 digestion. (**B**) Same sample after heating at 850°C for 30 min. Spinning sidebands are indicated by SSB; stishovite by ST.

J. F. McHone, Department of Geology, Arizona State University, Tempe, AZ 85287.
R. A. Nieman, C. F. Lewis, A. M. Yates, Department of Chemistry, Arizona State University, Tempe, AZ 85287.

Conventionally, X-ray diffraction (XRD) has been used to detect (*8*) stishovite in insoluble residues from quartz-rich samples digested in aqueous HF (*9*). This method has several disadvantages: the procedure is destructive, glasses possibly containing tetrahedrally or octahedrally coordinated silicon are preferentially destroyed, polymorphs formed in microscopic granules can be lost during concentration or may be too small for effective analysis and, in the presence of multiple mineral species, XRD peak positions may be superimposed and difficult to identify. Workers using XRD have been unable to detect stishovite conclusively in K-T boundary samples, although its presence has been suggested (*2*).

Stishovite can also be identified with high-resolution solid-state ^{29}Si magic-angle spinning (MAS) nuclear magnetic resonance (NMR) spectroscopy (*10*). The chemical shifts of silicon-bearing minerals, relative to tetramethylsilane (TMS), are strongly influenced by the coordination number of silicon in a solid: the shift for tetrahedrally coordinated silicon ranges from -60 to -121 ppm, whereas the shift for octahedrally coordinated silicon signals ranges from -171 to -223 ppm (*11*). Stishovite produces a narrow resonance at -191.3 ppm with an unusually short relaxation time (*10, 12*); ^{29}Si MAS NMR has been used successfully to identify stishovite in naturally shocked rocks from Barringer (Meteor) Crater, Arizona (*12*), and Vredefort Ring, South Africa (*13*).

We collected three samples (about 8 kg each) of boundary clay layer and up to 2 cm of overlying coal-rich clays from the Raton K-T boundary site, Raton, New Mexico (*14*), to search for stishovite. The samples were washed repeatedly for a period of several weeks in a lapidary tumbler with distilled water until no visible material remained in suspension. This procedure also partially disaggregated the samples and removed indurated clays. Residual grains were oven dried at 90°C, then ultrasonically cleansed for several days in distilled water. At daily intervals, samples were rinsed and allowed to settle, and samples were decanted until rinse waters were clear. The resulting samples were then dried and passed repeatedly through a Frantz magnetic separator (*15*). Non-magnetic fractions were again subjected to ultrasonic washing until wash waters were clear of suspended clay (mostly nacrite). Mostly coal fragments, feldspars, and quartz remained. We removed most of the coal by selective siphoning during vortex concentration. The residual material was treated at 80°C with concentrated nitric acid for 3 hours in order to remove those coal and lignite particles adhering to minute quartz growths. The resulting stained solution was oxidized by the slow addition of 30% hydrogen peroxide until all color vanished. Remaining grains (about 8 g from each sample) were washed in acetone and dried, then gently ground under distilled water for NMR and XRD studies. This separation process required 11 weeks. The separations were carried out with fresh glassware in a room that had never been previously used for stishovite isolation. The magnetic separator was dismantled and cleaned before use; NMR rotors were cleaned by sonification.

In the ^{29}Si MAS NMR spectrum of a split of mineral grains separated from one sample of the K-T boundary layer [Fig. 1A (*16*)], several resonances in the -80 to -110 ppm region resulting from feldspars, quartz, and possibly glasses containing tetrahedrally coordinated silicon were evident (Table 1). These same phases have been shown by XRD to dominate the bulk of this sample.

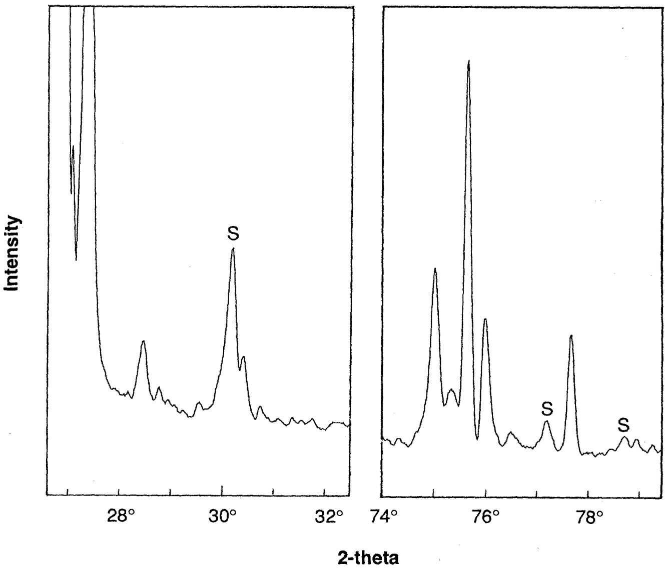

Fig. 2. Portions of an XRD powder pattern of HF-treated K-T boundary mineral grains. Data were obtained over a 2-theta range of 3° to 90° with a Rigaku D/Max-IIB automated diffractometer operated in summation step-scan mode and fitted with a "zero-background" quartz plate sample holder and a copper anode x-ray tube (Cu Kα_1 = 1.5406 Å); S indicates peaks due to stishovite.

Table 1. Assignment of ^{29}Si MAS NMR resonances (*11*) from K-T boundary mineral grains, Raton Pass, New Mexico.

Observed Chemical Shift (ppm)	Mineral
−92.6	Albite
−94.5	Microcline
−96.7	Albite and microcline
−100.3	Microcline
−104.6	Albite
−107.2	Quartz
−191.0	Stishovite

Table 2. Identification of stishovite with XRD; I/I$_1$ is intensity of peak relative to highest peak.

Reported (*18*)		Observed		Interfering mineral
d (Å)	*I*/*I*$_1$	*d* (Å)	2-theta (degrees)	
2.959	100	2.957	30.20	
2.246	18	2.247	40.10	
2.090	1	2.087	43.32	
1.981	35	1.980	45.78	quartz
1.870	14	1.869	48.68	
1.530	50	1.530	60.44	
1.478	18	1.481	62.68	rutile, anatase, zircon
1.333	10	1.339	70.24	anatase
1.322	4			
1.291	2	1.293	73.16	zircon
1.235	25	1.235	77.20	
1.215	10	1.215	78.68	
1.185	2	1.184	81.18	quartz
1.159	8	1.161	83.10	anatase
1.123	8	1.123	86.82	

In addition to these NMR resonances in our sample, a smaller sharp peak was evident with a chemical shift of -191.0 ppm (Fig. 1A). This peak is within the resonance range for octahedrally coordinated silicon and is in excellent agreement with the shift of -191.0 to -192.4 ppm that has been reported for natural stishovite (*10, 12, 13*). The narrow line width is also consistent with the presence of silicon in a crystalline as opposed to glassy phase. The same sample was then heated to 850°C for 30 min, air cooled, and reexamined with NMR (Fig. 1B). In this spectrum, the four-coordinated resonances in the -80 to -110 ppm region have begun to broaden and merge in the manner reported for heat-treated feldspars (*17*). Significantly, the resonance at -191.0 ppm vanished. Stishovite is easily destroyed by heat, and at temperatures as low as 300°C reverts to glass or cristobalite (*5, 7*). Therefore, the loss of the -191.0 ppm resonance upon heating is consistent with the presence of thermally metastable stishovite.

Natural stishovite has 14 reported XRD peaks between 3° and 90° 2-theta (*18*).

When the unheated mineral grains were examined with XRD, none of these peaks could be conclusively identified. Therefore, the remaining unheated portion of the sample showing the stishovite NMR peak was subjected to further acid treatment on a steambath. The sample was first digested 24 hours in 1:1 HNO_3, followed by 24 hours in 1:1 HCl and a small amount of solid ethylenediaminetetraacetic acid, which reduces precipitation of unwanted calcium and magnesium fluorides during HF treatment. Residual granules were twice partially digested in 1:1 HF in an open platinum dish and dried on a steambath. An XRD pattern of these final insoluble grains indicated the presence of quartz, rutile, anatase, and zircon. Furthermore, eight clearly observed XRD peaks (Fig. 2) have the *d*-spacings of stishovite (Table 2).

The combination of both ^{29}Si MAS NMR and XRD data demonstrate that stishovite occurs in the K-T boundary layer at Raton, New Mexico. Both NMR and powder XRD are bulk analytical techniques; neither method can determine precise size nor location of phases in a sample. However, two potential stishovite precursor materials, zircon and quartz, occur in the boundary layer at Raton and in K-T boundary deposits at Clear Creek North, Colorado (*19*). Transmission electron microscope studies of Clear Creek quartz grains have shown that shock lamellae contain glassy material that, unlike natural heat-fused silica (lechatelierite), appears to be slightly denser than surrounding host quartz (*19*). At the Ries impact structure in Germany, stishovite has been reported in diaplectic (glassy) quartz shock lamellae (*20*). If stishovite in the Raton K-T boundary layer is formed from quartz rather than zircon, it may occur in these dense glassy lamellae.

Comparison with other ^{29}Si-MAS NMR spectra obtained in our laboratory suggests that the K-T boundary grains in the NMR split contained 1 to 3 mg of stishovite. Therefore, we estimate that from 16 to 48 mg of stishovite was in the 8 g of material separated from the original 8 kg sample. We were unable to determine the proportion of stishovite to other mineral phases in the K-T boundary sample. Stishovite, because of its short relaxation time, can be detected with enhanced sensitivity relative to other mineral phases (*10, 12*). The long recycle delays needed for more quantitative measurements would seriously degrade the sensitivity to stishovite.

At known impact structures, coesite commonly occurs in the same rocks as stishovite (*8, 20*). However, coesite cannot always be observed in samples from these sites, even where stishovite is present at concentrations greater than 0.5% relative to primary quartz. Coesite was also not observed in stishovite-bearing samples from laboratory shock experiments (*21*). During our study, three similar samples (about 8 kg each) of boundary material were processed and examined. Coesite could not be detected, and stishovite was observed in all splits from only one sample. Our results indicate that stishovite is unevenly distributed within K-T boundary deposits and occurs in very small amounts. Even when found in situ at thoroughly studied impact structures, silica pressure polymorphs are rare and occurrences are sporadic. Detection of stishovite is strong evidence that shocked components in K-T boundary sediments result from extraterrestrial impact: it is thermally unstable at moderate pressures and should not survive the prolonged heat of a near surface volcanic event.

REFERENCES AND NOTES

1. L. W. Alvarez, W. Alvarez, F. Asaro, H. V. Michel, *Science* **208**, 1095 (1980).
2. B. F. Bohor *et al.*, *ibid.* **224**, 867 (1984).
3. B. F. Bohor *et al.*, *ibid.* **236**, 705 (1987).
4. A. Hallam, *ibid.* **238**, 1237 (1987).
5. S. M. Stishov and S. V. Popova, *Geochemistry* **10**, 923 (1961).
6. K. Kusaba, Y. Syono, M. Kikuchi, K. Fukuoka, *Earth Planet. Sci. Lett.* **72**, 443 (1985).
7. B. J. Skinner and J. J. Fahey, *J. Geophys. Res.* **68**, 5595 (1963).
8. S. W. Kieffer, *ibid.* **76**, 5449 (1971); ———, P. P. Phakey, J. M. Christie, *Contrib. Mineral. Petrol.* **59**, 41 (1976).
9. J. J. Fahey, *Am. Mineral.* **49**, 1643 (1964).
10. J. V. Smith and S. C. Blackwell, *Nature* **303**, 223 (1983); J. M. Thomas, J. M. Gonzalez-Calbert, C. A. Fyfe, G. C. Gobbi, M. Nicol, *Geophys. Res. Lett.* **10**, 91 (1983).
11. K. A. Smith, R. J. Kirkpatrick, E. Oldfield, D. M. Henderson, *Am. Mineral.* **68**, 1206 (1983); G. Engelhardt and D. Michel, *High-Resolution Solid-State NMR of Silicates and Zeolites* (Wiley and Sons, New York, 1987); R. Dupree, D. Holland, M. G. Mortuza, *Nature* **328**, 416 (1987).
12. W.-H. Yang *et al.*, *Meteoritics* **21**, 117 (1986).
13. J. McHone and R. A. Nieman, *ibid.* **23**, 289 (1988).
14. C. L. Pillmore and R. M. Flores, *Geol. Soc. Am. Spec. Pap. 209* (1987). Stratigraphy described in detail for site located at latitude 36°54′12″N, longitude 104°27′04″W.
15. Frantz settings: 10° down-slope, 5° tilt (magnetic up), 1.5 ampere current.
16. Spectra were obtained with a Bruker AM-400 spectrometer equipped with a multinuclear MAS probe operating at 79.5 MHz for ^{29}Si. Samples (450–500 mg) were spun at 4.5 to 5.2 KHz in single air-bearing Delrin rotors. The magic angle was adjusted by maximizing spinning side-bands of the ^{79}Br resonance in KBr, and chemical shifts were referenced to external TMS and are reproducible to about ±0.3 ppm. Magnetic field drift was compensated to better than 0.5 ppm per day. Free induction decays (15,000 to 60,000) were acquired over a period of 1 to 3 days for a spectral width of 35,714 Hz, an acquisition time of 115 ms, a 75° pulse width, and a delay of 5 s between acquisitions.
17. B. L. Sherriff and J. S. Hartman, *Can. Mineral.* **23**, 205 (1985).
18. E. C. T. Chao, J. J. Fahey, J. Littler, D. J. Milton, *J. Geophys. Res.* **67**, 419 (1962).
19. A. Gratz *et al.*, *Lunar Planet. Sci. XIX*, 419 (1988).
20. D. Stoffler, *J. Geophys. Res.* **76**, 5474 (1971).
21. P. S. De Carli and D. J. Milton, *Science* **147**, 144 (1965).

22. The work of J.F.M. was partially supported by R. S. Dietz and Barringer Crater Company, Princeton, New Jersey. We thank T. I. Emilsson and C. L. Pillmore for helpful discussions. Samples were collected with the assistance of M. R. Owen. The NMR spectrometer was purchased with assistance from Arizona State University and National Science Foundation grant CHE-8409644.

11 November 1988; accepted 19 January 1989

Sequence-Specific Peptide Cleavage Catalyzed by an Antibody

BRENT L. IVERSON AND RICHARD A. LERNER

Monoclonal antibodies have been induced that are capable of catalyzing specific hydrolysis of the Gly-Phe bond of peptide substrates at neutral *p*H with a metal complex cofactor. The antibodies were produced by immunizing with a Co(III) triethylenetetramine (trien)–peptide hapten. These antibodies as a group are capable of binding trien complexes of not only Co(III) but also of numerous other metals. Six peptides were examined as possible substrates with the antibodies and various metal complexes. Two of these peptides were cleaved by several of the antibodies. One antibody was studied in detail, and cleavage was observed for the substrates with the trien complexes of Zn(II), Ga(III), Fe(III), In(III), Cu(II), Ni(II), Lu(III), Mg(II), or Mn(II) as cofactors. A turnover number of 6 × 10^{-4} per second was observed for these substrates. These results demonstrate the feasibility of the use of cofactor-assisted catalysis in an antibody binding site to accomplish difficult chemical transformations.

MONOCLONAL ANTIBODIES HAVE been elicited that can catalyze a number of chemical reactions, including ester (*1*) or carbonate (*2*) hydrolysis, a stereospecific lactonization reaction (*3*), bimolecular amide formation (*4*), a stereospecific Claisen rearrangement (*5*), hydrolysis of a *p*-nitroanilide amide (*6*), and a photochemical cleavage of thymine dimers

---

Department of Molecular Biology, The Research Institute of Scripps Clinic, La Jolla, CA 92037.